Calculating Magnetic Permeability Response of a Conducting Square Ring Structure

Amir Khodamohammadi[a,*], Ahmad Khayat Jafari[b], and Reza Aghbolaghi[c]

[a]Department of Physics, Bonab Branch, Islamic Azad University, Bonab, 55518-134, Iran
[b]Department of Physics, University of South Florida, Tampa, Florida, 33620, USA
[c]Department of Physics, University of Bonab, Bonab 55517 Iran

[*]Corresponding Author Email: a_k_mohammadi@yahoo.com

ABSTRACT— In the present work, we investigate the tunability of the magnetic response of a new structure. A lattice of periodically arranged close-packed square conducting rings has been studied for this purpose. Here, instead of enhancing the magnetic activity via resonance, like in split-ring resonators, we concentrate on the analysis of the interactions between these rings. The core idea is to design an array with negligible capacity and to focus on inductive interactions between its building cells. In other words, in this structure, the enhancement of the microscopic process has been attained by the interaction of its building block, i.e. a collective feature has been considered. It is our goal to obtain a sizable magnetic response with this new approach. Our ultimate goal is to demonstrate that the relative magnetic permeability of this architecture could be less than one or even less than zero.

KEYWORDS: Magnetic permeability; meta-material; antiferromagnetic coupling; mutual inductance; self-inductance

I. INTRODUCTION

In recent years new concepts in synthesis and novel fabrication techniques have allowed the construction of structures and composite materials that have new response functions do not occur in nature. Meta-materials are by definition composites, whose properties are not determined by the fundamental physical properties of their constituents but by the shape and distribution of specific patterns included in them. Thus for certain patterns and distribution, the measured effective permittivity ε_{eff} and the effective permeability μ_{eff} can be made to be less than zero. In such materials, the phase and group velocity of an electro-magnetic wave propagate in opposite directions giving rise to fascinating new outcomes for a number of laws of physics [1]-[4].

Electromagnetic wave propagation in left handed materials (LHMs) has been studied both analytically and numerically [5]. In order to model LHM numerically, the robust finite-difference time-domain (FDTD) method has been employed. The FDTD method has been proved to be one of the most effective numerical methods in the study of LHM. Since it is a time domain solver, it is convenient for dealing with the characteristics of LHMs over a wide frequency band. FDTD approach not only supports the steady state phenomena associated with the frequency domain analysis, but also demonstrates the causal transient behaviors [6], [7].

In fact, LHM are formations of two different substructures. One of them addresses the electric response and the other one provides the magnetic response. There have been many investigations and successful experimental realizations for both substructures [3], [4]. Although most materials exhibiting a good electric response can be found at almost any frequency from radio-frequencies to the ultraviolet frequencies, the magnetic response of most materials is limited to low microwave frequencies and therefore the relative magnetic permeability can be fixed to $\mu_r = 1$. Any magnetization effects tend to abate beyond the gigahertz frequency range. It is a real

challenge for researchers all over the world to create any magnetic activity at optical frequencies and, in addition, reaching for values $\mu_r<1$ [3]. Those materials, such as the ferrites, that remain moderately active are often heavy, and may not have very desirable mechanical properties [8]. Some ferromagnetic, ferrimagnetic and antiferromagnetic materials exhibit some magnetic activity at even frequencies of hundreds of gigahertz [9]-[11]. But these are rare and usually have narrow bandwidths. In fact, Landau and Lifshitz gave a very general argument as to how the magnetic activity arising from atomic orbital currents should be negligible at optical frequencies if one could neglect the polarization currents [12].

This behavior can be explained with the conditions for the occurrence of magnetic activity. In general, magnetic polarization appears from either unpaired electron spins or orbital electron currents, and the collective excitations of these usually tend to occur at low frequencies. The first effect cannot be used at optical frequencies as the time scale of spins interacting with radiation is much larger than the time scales of processes at optical frequencies. For the second effect one tries to create a closed current that generates a magnetic moment opposed to the incoming magnetic field. Since we speak of length scales of a fraction of the optical wavelength, those current rings are very small and so is their magnetization [3].

The challenge to produce a meta-material with a considerable magnetic response has resulted in the design of spilt-ring and other resonant structures. By introducing capacitive elements into the system, a rich resonant response can be induced [3]. This has become well-known subsequently as the split-ring resonator (SRR). The SRR works on the principle that the magnetic field of the electromagnetic radiation can drive a resonant L-C circuit through the inductance. This results in a dispersive effective magnetic permeability. The SRRs are the basis of most of the meta-materials exhibiting negative magnetic permeability today [3], [8], [13]-[15]. Nonlinear properties of two-dimensional arrays of wires and split-ring resonators embedded into a nonlinear dielectric have also been calculated [16]. However, it still remains difficult to manufacture such small metallic patterns without losing the effect due to absorption. Many groups have been trying to overcome this detrimental effect with resonance but they have encountered problems due to high absorption [17].

The present work utilizes second approach. We are going to focus on the potential of the circulating currents in the current research. These currents produce a magnetic moment opposing the incident magnetic field. The magnetic moment of every single building block contributes to the magnetization of the entire composite. It is expected that the magnetic response of this formation to be smaller than the one from a resonant structure. The interactions between the constituents have been neglected in most of the work on meta-materials, although they make an important contribution to the magnetic properties [18].

In order to obtain the macroscopic properties of the configuration, we have to analyze the microscopic processes of self- and mutual inductance of two- and three-dimensional ring system. So the self- and total mutual inductance of our design has to be calculated in the first step. Then, we apply a suitable averaging procedure to make appropriate predictions about the magnetic response of the structure.

II. THEORY

As revealed earlier, manipulating the magnetic response proves to be the more challenging task. As there is a wide range of values for ε existing in nature, it is easier to engineer composites with the desired electrical response compared to the magnetic one. In this paper, we disregard the electric response and its substructure [19], [20] (relevant researches can be found in elsewhere [3]) and concentrate on the possibilities to vary the magnetic properties of an artificial material.

LHMs are strictly distinguished from other structured photonic materials, i.e. photonic crystals (PCs) or photonic band-gap (PBG) materials. In these materials the band-gaps arise as a result of multiple Bragg scattering in a periodic array of dielectric scatterers. The periodicity of the architecture here is of the order of the wavelength, and hence homogenization in this sense cannot be carried out. On the other hand, in LHMs the periodicity is by comparison far less important and all the properties mainly depend on the single scatterer resonances [3]. Thus there is a restriction on the dimensions of the building blocks of LHM. If we are concerned about the response of the system to electromagnetic radiation of frequency ω, the necessary conditions are defined as follows:

$$D \ll \lambda = \frac{2\pi c}{\omega} \tag{1}$$

where c is the velocity of electromagnetic wave in the medium and D is the lattice constant. If this condition were not obeyed, there would be the possibility that internal structure of the medium could diffract as well as refract radiation. Long wavelength radiation is too myopic to detect internal structure and, in this limit, an effective permittivity, and permeability is a valid concept [8]. If the retardation effects are taken into account, there will not be any restriction to the long wavelength limit. Consequently, the basic elements could have a size comparable to the wavelength which in turn simplifies the fabrication of a construction having a magnetic response at optical frequencies [18].

To start with we consider an array of N conducting rings. They are arranged in a plane (two-dimensional x-y plane) and their symmetry axis is oriented along the z-axis. We are going to investigate square lattice architecture since it fulfills our requirements with respect to flux capture better than other structures. Several layers of these flat rings may be stacked periodically in a dielectric material (three-dimensional) that ensures the correct spacing between the layers. This spacing determines the packing density of the induced magnetic moments, which is as important for the response of the construction as the strength of the magnetic interactions [18], [21], [22].

By the accurate calculation of the interaction between the rings, we are able to derive the expression for the magnetic response of the entire system. The effective magnetic susceptibility χ_m can be obtained from the averaged macroscopic magnetization $\vec{M}$. The details of this calculation have been presented in reference [18], [22]. Moreover, modeling and numerical calculations for the various circular ring arrangements have been elaborated there. Here, we are modeling the square ring formation. The magnetic flux enclosed by a square ring lattice is the most due to the fact that there is no gap between the squares as depicted in Fig. 1. Therefore the interactions between the squares should be stronger and lead to a mutual inductance that is more negative than for circles. We also compare the similar properties of the circular and the square ring formation together and demonstrate that the latter show more favorite magnetic response.

Because this arrangement is isotropic, we can employ the scalar form of the equation for the magnetic susceptibility of the structure:

$$\chi_m = \frac{\partial \mathcal{M}}{\partial H} = -\mu_0 \frac{A_{ring}^2}{v} \frac{1}{L + \bar{M} + i\dfrac{R}{\omega}} = \tag{2}$$

$$-\mu_0 \frac{A_{ring}^2}{v} \left[\frac{\left(L + \bar{M}\right) - i\dfrac{R}{\omega}}{\left(L + \bar{M}\right)^2 + \left(\dfrac{R}{\omega}\right)^2} \right]$$

where A_{ring} is the area of the ring, v is the volume of a primitive cell which holds only one ring inside, $\bar{M}$ is the total mutual inductance, L and R are the self-inductance and the resistance of the circuit, respectively. In this final expression, the significant role of the interaction between the rings becomes obvious via the total mutual inductance of the composite $\bar{M}$.

The self-inductance L is always positive. The mutual inductance M between two square rings can either be positive or negative, depending whether we have anti-ferromagnetic or ferromagnetic interactions between the rings. In general, the absolute value of the mutual inductance is not larger than the self-inductance $L > |\bar{M}|$. Hence in Eq. (2), the magnetic susceptibility χ_m is negative and it is concluded that the magnetic response of our ring lattice is diamagnetic.

By amplifying the ferromagnetic interactions between the rings, it is possible to enhance the absolute value of the total mutual inductance of the structure. This, in turn, leads to an increase of the magnitude of the magnetic susceptibility.

The effective magnetic permeability μ_{eff} and the susceptibility χ_m are linked through the following relation [23], [24]:

$$\mu = \mu_0 \mu_r = \mu_0 (1 + \chi_m) = \mu_0 \left(1 - \mu_0 \frac{A_{ring}^2}{v} \frac{1}{L + \bar{M} + i \frac{R}{\omega}} \right) = \mu_0 \left\{ 1 - \mu_0 \frac{A_{ring}^2}{v} \left[\frac{\left(L + \bar{M} \right) - i \left(\frac{R}{\omega} \right)}{\left(L + \bar{M} \right)^2 + \left(\frac{R}{\omega} \right)^2} \right] \right\} \quad (3)$$

Pendry *et al*. have proposed a structure made of an array of long cylinders where one could neglect the interaction between them [8]. It is possible to reproduce their results by setting the total mutual inductance $\bar{M} = 0$ and utilize the expression for the self-inductance of a long solenoid. Within this framework μ_r is always in the range $0 \leq \mu_r \leq 1$. As an inference from this fact the authors of reference [8] concluded that a resonant enhancement is needed to access the desired values for the negative permeability $\mu_r \leq 0$. This diamagnetic screening effect has been known for superconducting cylindrical shells [23], and a diamagnetic effective medium is also obtained with percolation metallo-dielectric composites [25].

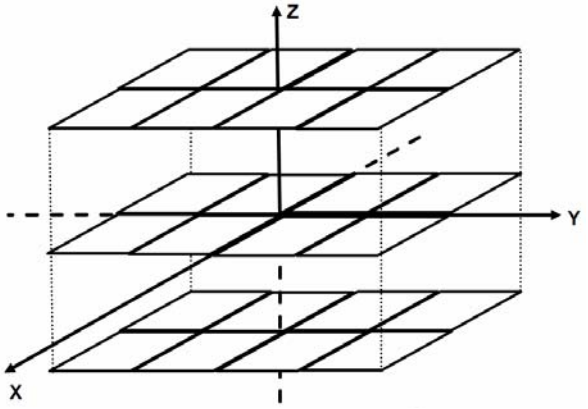

Fig. 1. There is no magnetic flux loss in a square ring lattice in three-dimension. Any other geometry like circles has some flux loss due to the fact that there is gap between the building blocks even in the most compact arrangement.

On the other hand, taking the mutual inductance into account, as we are doing in this work, has major consequences for the physical outcome of our proposed architecture [18], [22].

III. NUMERICAL APPROACH

A. Mutual inductance

Firstly, we describe the calculation of the mutual inductance M_{ij} between two infinitesimal square thin rings. The coefficient M_{ij} between two distinct current-carrying circuits is given by the following formula [23]:

$$M_{ij} = M_{ji} = \frac{\mu_0}{4\pi I_i I_j} \int_{C_i} dV_i \int_{C_j} \frac{\vec{J}(\vec{r}_i) \cdot \vec{J}(\vec{r}_j')}{|\vec{r}_i - \vec{r}_j'|} dV_j' \quad (4)$$

If the circuits are imagined to be negligible in cross-section compared to the overall scale of both circuits, the following integral is obtained:

$$M_{ij} = M_{ji} = \frac{\mu_0}{4\pi} \oint_{C_i} \int_{C_j} \frac{d\vec{l}_i \cdot d\vec{l}_j}{|\vec{r}_i - \vec{r}_j|} = \frac{\mu_0}{4\pi} \oint_{C_i} d\vec{l}_i \cdot \oint_{C_j} \frac{d\vec{l}_j}{|\vec{r}_i - \vec{r}_j|} \quad (5)$$

which is known as Neumann's formula for the mutual inductance [23].

We consider two squares in x-y plane with arbitrary position. Note that they should not be

tilted against each other nor overlap. Otherwise they cannot be put beside each other and fill the x-y plane with any void. For simplicity, it is supposed that one of the squares is located on the reference point. This model is indicated schematically in Fig. 2.

In the graphs, all of the involved parameters are scaled with the length of the side of the square a. Neumann formula for calculating the mutual inductance between these two squares has the following form:

$$M_{12}^{2D} = \frac{\mu_0}{4\pi}\Bigg[\int_{y_1=0}^{y_1=a}\int_{y_2=D\sin\propto}^{y_2=D\sin\propto+a} \frac{dy_1 dy_2}{\left[(y_1-y_2)^2+(D\cos\propto)^2\right]^{1/2}} + \int_{y_1=0}^{y_1=a}\int_{y_2=D\sin\propto+a}^{y_2=D\sin\propto} \frac{dy_1 dy_2}{\left[(y_1-y_2)^2+(D\cos\propto+a)^2\right]^{1/2}} + \int_{x_1=0}^{x_1=a}\int_{x_2=D\cos\propto}^{x_2=D\cos\propto+a} \frac{dx_1 dx_2}{\left[(x_2-x_2)^2+(D\sin\propto)^2\right]^{1/2}} + \int_{x_1=0}^{x_1=a}\int_{x_2=D\cos\propto+a}^{x_2=D\cos\propto} \frac{dx_1 dx_2}{\left[(x_1-x_2)^2+(D\sin\propto-a)^2\right]^{1/2}} + \int_{y_1=a}^{y_1=0}\int_{y_2=D\sin\propto}^{y_2=D\sin\propto+a} \frac{dy_1 dy_2}{\left[(y_1-y_2)^2+(D\cos\propto-a)^2\right]^{1/2}} + \int_{y_1=a}^{y_1=0}\int_{y_2=D\sin\propto+a}^{y_2=D\sin\propto} \frac{dy_1 dy_2}{\left[(y_1-y_2)^2+(D\cos\propto)^2\right]^{1/2}} + \int_{x_1=a}^{x_1=0}\int_{x_2=D\cos\propto}^{x_2=D\cos\propto+a} \frac{dx_1 dx_2}{\left[(x_1-x_2)^2+(D\sin\propto+a)^2\right]^{1/2}} + \int_{x_1=a}^{x_1=0}\int_{x_2=D\cos\propto+a}^{x_2=D\cos\propto} \frac{dx_1 dx_{j2}}{\left[(x_1-x_2)^2+(D\sin\propto)^2\right]^{1/2}} \Bigg] \quad (6)$$

The results have been delineated in Figs. 3 and 4. In Fig. 3 the mutual inductance of the squares has been shown versus their position with respect to each other. An oscillatory (repetitive pattern) behavior is observed in this figure. This behavior is expected due to the symmetry of the mutual inductance between squares. In Fig. 4 the mutual inductance is depicted against the distance between two squares. As the distance increases, the magnitude mutual inductance decreases. We expect this behavior according to the Neumann equation.

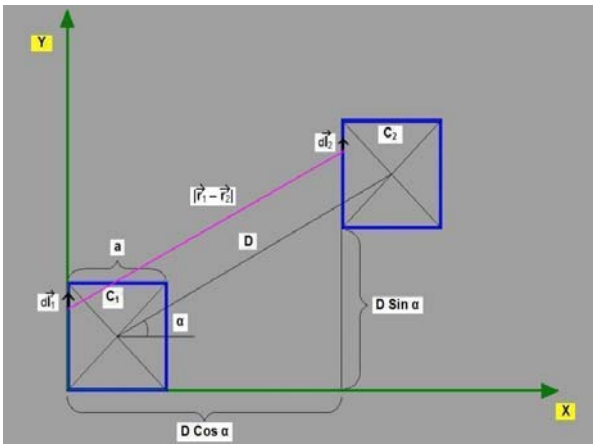

Fig. 2. In this figure, all of the necessary parameters for numerical calculation of the mutual inductance between two infinitesimal thin conducting square rings have been shown.

In the next step, the case of a lattice made up from these square rings is being analyzed. For such an array, the mutual inductance between all the rings should been calculated simultaneously. Since we have assumed that our problem is linear, the electromagnetic fields could be superposed. We must accumulate all the contributions from neighboring rings relative to the ring of reference (ring zero) [18].

For two-dimension case, we lay square ring cells in a flat surface like tiles according to Fig. 5. The appropriate coordinate system for the square rings is the Cartesian coordinate system compared to spherical one for the circular rings [18]. The lattice vector $\vec{R}$ determines the distance between the center of the reference ring and the neighboring rings. It can be expressed with the unit vectors in $\hat{i}$ and $\hat{j}$ direction:

$$\vec{R} = n_i D\hat{i} + n_j D\hat{j} \quad (7.a)$$

$$\left|\vec{R}\right| = D\sqrt{n_i^2 + n_j^2} \quad (7.b)$$

where the lattice constant is denoted with D.

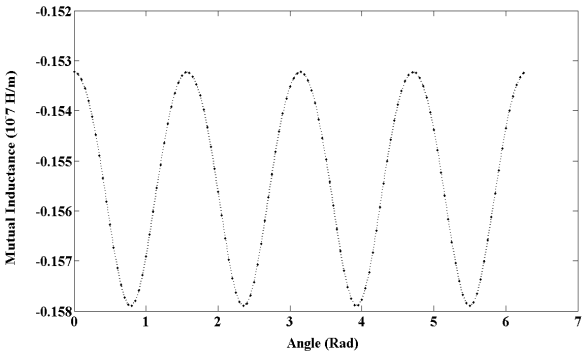

Fig. 3. The mutual inductance of two squares against their position with respect to each other. In this case, the distance between two squares is constant (D/a=2) and one of them rotates around another one. Its oscillatory behavior is due to the symmetry of the mutual inductance between two squares.

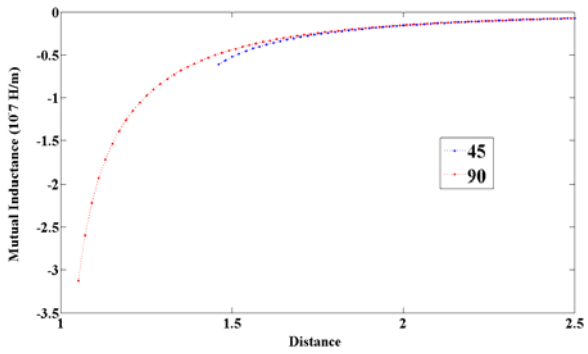

Fig. 4. The mutual inductance of two conducting square rings versus the distance between the center of them. In one case, the angle between squares is 45° and in another one is 90°. When the angle is 45°, the closest distance is $\sqrt{2}a \simeq 1.4a$.

Now we can calculate the mutual inductance between the reference square ring and the other ones individually and take the sum over all contributions characterized by different vectors $\vec{R}$:

$$\bar{M}_{2D} = \sum_{n_i=-\infty}^{n_i=+\infty} \sum_{n_j=-\infty}^{n_j=+\infty} M_{12}^{2D}\left(n_i, n_j\right) \qquad (8.a)$$

where $M_{12}^{2D}(n_i,n_j)$ is obtained by the following integrations:

$$M_{12}^{2D}\left(n_i, n_j\right) = \frac{\mu_0}{4\pi}\left[\int_{y_1=0}^{y_1=a} \int_{y_2=n_jD}^{y_2=n_jD+a} \frac{dy_1 dy_2}{\left[\left(y_1-y_2\right)^2+\left(n_iD\right)^2\right]^{1/2}} + \right.$$

$$\int_{y_1=0}^{y_1=a} \int_{y_2=n_jD+a}^{y_2=n_jD} \frac{dy_1 dy_2}{\left[\left(y_1-y_2\right)^2+\left(n_iD+a\right)^2\right]^{1/2}} +$$

$$\int_{x_1=0}^{x_1=a} \int_{x_2=n_iD}^{x_2=n_iD+a} \frac{dx_1 dx_2}{\left[\left(x_1-x_2\right)^2+\left(n_jD\right)^2\right]^{1/2}} +$$

$$\int_{x_1=0}^{x_1=a} \int_{x_2=n_iD+a}^{x_2=n_iD} \frac{dx_1 dx_2}{\left[\left(x_1-x_2\right)^2+\left(n_jD-a\right)^2\right]^{1/2}} +$$

$$\int_{y_1=a}^{y_1=0} \int_{y_2=n_jD}^{y_2=n_jD+a} \frac{dy_1 dy_2}{\left[\left(y_1-y_2\right)^2+\left(n_iD-a\right)^2\right]^{1/2}} +$$

$$\int_{y_1=a}^{y_1=0} \int_{y_2=n_jD+a}^{y_2=n_jD} \frac{dy_1 dy_2}{\left[\left(y_1-y_2\right)^2+\left(n_iD\right)^2\right]^{1/2}} +$$

$$\int_{x_1=a}^{x_1=0} \int_{x_2=n_iD}^{x_2=n_iD+a} \frac{dx_1 dx_2}{\left[\left(x_1-x_2\right)^2+\left(n_jD+a\right)^2\right]^{1/2}} +$$

$$\left. \int_{x_1=a}^{x_1=0} \int_{x_2=n_iD+a}^{x_2=n_iD} \frac{dx_1 dx_2}{\left[\left(x_1-x_2\right)^2+\left(n_jD\right)^2\right]^{1/2}} \right] \qquad (8.b)$$

By adding every contribution from any ring in the x-y plane, we derive the total mutual inductance $\bar{M}_{2D}$ induced in the reference cell. As the arrangement is periodic, one reaches the conclusion that choosing another ring of reference will also lead to the same result. The sum over the different contributions in Eq. (8a) is symmetric. When we take a finite amount of neighbors into account, the summation becomes asymmetric. The total mutual inductance depending on the number of included neighbors is plotted in Fig. 6. It is seen that the sum for the total mutual inductance converges for the summation over the finite number of the neighboring cells.

For an array of rings in three-dimension, the separation of the rings in the z-direction is characterized by the height of H. In contrast to the two-dimensional case, ferro- and anti-ferromagnetic coupling between the rings has

to be considered in the three-dimensional structures.

There are different pattern of stacking of layers. Here, we only consider two types of stacking: ordinary layer stacking (AA stacking) and every other layer stacking (AB stacking). Accordingly we define two different lattice vectors $\vec{R}_A$ and $\vec{R}_B$.

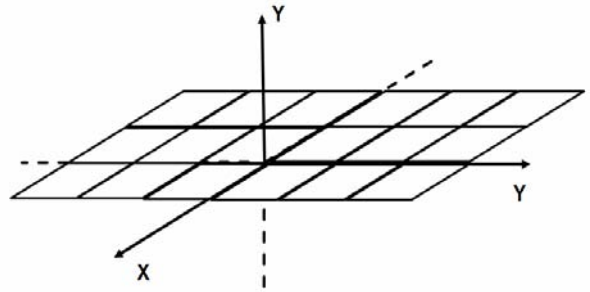

Fig. 5. Two-dimensional arrangement of the square ring cells. The lattice extends in both x and y direction.

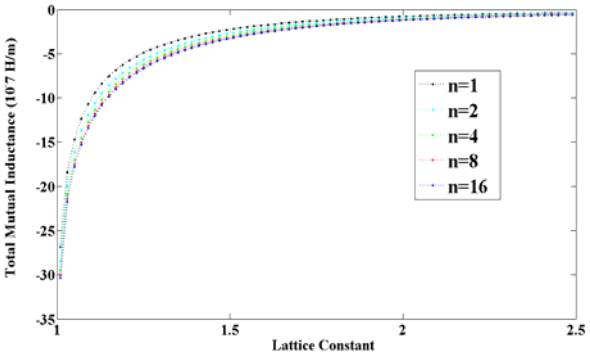

Fig. 6. The total mutual inductance versus the distance between cells. The number of neighbors has also been shown. It is seen that the total mutual inductance converges enough for 16 neighbors.

First, as shown in Fig. 7, AA stacking is taken into account. We define the three-dimensional vector $\vec{R}_A$ as follows:

$$\vec{R}_A = n_i D\hat{i} + n_j D\hat{j} + n_k H\hat{k} \qquad (9.a)$$

$$\left|\vec{R}_A\right| = D\left[n_i^2 + n_j^2 + n_k^2 \left(H/D\right)^2\right]^{1/2} \qquad (9.b)$$

The lattice vector for AB stacking, as illustrated in Fig. 8, is defined by the following relations:

$$\vec{R}_B = \left(n_i + \frac{1}{2}\right)D\hat{i} + \left(n_j + \frac{1}{2}\right)D\hat{j} + n_k H\hat{k} \qquad (10.a)$$

$$\left|\vec{R}_B\right| = D\left[\left(n_i + \frac{1}{2}\right)^2 + \left(n_j + \frac{1}{2}\right)^2 + n_k{}^2\left(\frac{H}{D}\right)^2\right]^{1/2} = D\left[n_i^2 + n_j^2 + n_i + n_j + \frac{1}{2} + n_k{}^2\left(\frac{H}{D}\right)^2\right]^{1/2} \qquad (10.b)$$

The total mutual inductance of the structure $\overline{M}_{3D}$ is obtained by aggregating all contributions of the mutual inductances designated by different vectors $\vec{R}$:

$$\overline{M}_{3D} = \sum_{n_i=-\infty}^{n_i=+\infty}\sum_{n_j=-\infty}^{n_j=+\infty}\sum_{n_k=-\infty}^{n_k=+\infty} M_{12}^{3D}\left(n_i, n_j, n_k\right) \qquad (11)$$

First, AA stacking is considered. In order to obtain $\overline{M}_{3D}$ for this kind of array, only the A-layer contribution is taken into account:

$$\overline{M}_{3D}^{A} = \sum_{n_i=-\infty}^{n_i=+\infty}\sum_{n_j=-\infty}^{n_j=+\infty}\sum_{n_k=-\infty}^{n_k=+\infty} M_{12,A}^{3D}\left(n_i, n_j, n_k\right) \qquad (12.a)$$

where $M_{12,A}^{3D}\left(n_i, n_j, n_k\right)$ is obtained by the following integrations:

$$M_{12,A}^{3D}\left(n_i, n_j, n_k\right) = \frac{\mu_0}{4\pi}\Bigg[$$

$$\int_{y_1=0}^{y_1=a}\int_{y_2=n_jD}^{y_2=n_jD+a}\frac{dy_1dy_2}{\left[\left(y_1-y_2\right)^2+\left(n_iD\right)^2+\left(n_kH\right)^2\right]^{1/2}} +$$

$$\int_{y_1=0}^{y_1=a}\int_{y_2=n_jD+a}^{y_2=n_jD}\frac{dy_1dy_2}{\left[\left(y_1-y_2\right)^2+\left(n_iD+a\right)^2+\left(n_kH\right)^2\right]^{1/2}} +$$

$$\int_{x_1=0}^{x_1=a}\int_{x_2=n_iD}^{x_2=n_iD+a}\frac{dx_1dx_2}{\left[\left(x_1-x_2\right)^2+\left(n_jD\right)^2+\left(n_kH\right)^2\right]^{1/2}} +$$

$$\int_{x_1=0}^{x_1=a}\int_{x_2=n_iD+a}^{x_2=n_iD}\frac{dx_1dx_2}{\left[\left(x_1-x_2\right)^2+\left(n_jD-a\right)^2+\left(n_3H\right)^2\right]^{1/2}} +$$

$$\int_{y_1=a}^{y_1=0}\int_{y_2=n_jD}^{y_2=n_jD+a}\frac{dy_1dy_2}{\left[\left(y_1-y_2\right)^2+\left(n_iD-a\right)^2+\left(n_3H\right)^2\right]^{1/2}} +$$

$$\int_{y_1=a}^{y_1=0}\int_{y_2=n_jD+a}^{y_2=n_jD}\frac{dy_1dy_2}{\left[\left(y_1-y_2\right)^2+\left(n_iD\right)^2+\left(n_3H\right)^2\right]^{1/2}} +$$

$$\int_{x_1=a}^{x_1=0}\int_{x_2=n_iD}^{x_2=n_iD+a}\frac{dx_1dx_2}{\left[\left(x_1-x_2\right)^2+\left(n_jD+a\right)^2+\left(n_3H\right)^2\right]^{1/2}} +$$

$$\int_{x_1=0}^{x_1=a}\int_{x_2=n_jD}^{x_2=n_jD+a}\frac{dx_1dx_2}{\left[\left(x_1-x_2\right)^2+\left(n_jD\right)^2+\left(n_3H\right)^2\right]^{1/2}}\Bigg] \quad (12.b)$$

Second, AB stacking is considered. To obtain $\overline{M}_{3D}$ for this type of stacking, both B- and A-layer contributions should be included:

$$\overline{M}_{3D}^{B}=\sum_{n_i=-\infty}^{n_i=+\infty}\sum_{n_j=-\infty}^{n_j=+\infty}\sum_{n_k=-\infty}^{n_k=+\infty}\left[M_{12,A}^{3D}\left(n_i,n_j,n_k\right)+M_{12,B}^{3D}\left(n_i,n_j,n_k\right)\right] \quad (13.a)$$

The contribution of B-layers is calculated by the following integrals:

$$M_{12,B}^{3D}\left(n_i,n_j,n_k\right)=\frac{\mu_0}{4\pi}\Bigg[$$

$$\int_{y_1=0}^{y_1=a}\int_{y_2=\left(n_j+\frac{1}{2}\right)D}^{y_2=\left(n_j+\frac{1}{2}\right)D+a}\frac{dy_1dy_2}{\left\{\left(y_1-y_2\right)^2+\left[\left(n_i+\frac{1}{2}\right)D\right]^2+\left(n_kH\right)^2\right\}^{1/2}}+$$

$$\int_{y_1=0}^{y_1=a}\int_{y_2=\left(n_j+\frac{1}{2}\right)D+a}^{y_2=\left(n_j+\frac{1}{2}\right)D}\frac{dy_1dy_2}{\left\{\left(y_1-y_2\right)^2+\left[\left(n_i+\frac{1}{2}\right)D+a\right]^2+\left(n_kH\right)^2\right\}^{1/2}}+$$

$$\int_{x_1=0}^{x_1=a}\int_{x_2=\left(n_i+\frac{1}{2}\right)D}^{x_2=\left(n_i+\frac{1}{2}\right)D+a}\frac{dx_1dx_2}{\left\{\left(x_1-x_2\right)^2+\left[\left(n_j+\frac{1}{2}\right)D\right]^2+\left(n_kH\right)^2\right\}^{1/2}}+$$

$$\int_{x_1=0}^{x_1=a}\int_{x_2=\left(n_i+\frac{1}{2}\right)D+a}^{x_2=\left(n_i+\frac{1}{2}\right)D}\frac{dx_1dx_2}{\left\{\left(x_1-x_2\right)^2+\left[\left(n_j+\frac{1}{2}\right)D-a\right]^2+\left(n_kH\right)^2\right\}^{1/2}}+$$

$$\int_{y_1=0}^{y_1=a}\int_{y_2=\left(n_j+\frac{1}{2}\right)D}^{y_2=\left(n_j+\frac{1}{2}\right)D+a}\frac{dy_1dy_2}{\left\{\left(y_1-y_2\right)^2+\left[\left(n_i+\frac{1}{2}\right)D-a\right]^2+\left(n_kH\right)^2\right\}^{1/2}}+$$

$$\int_{y_1=a}^{y_1=0}\int_{y_2=\left(n_j+\frac{1}{2}\right)D+a}^{y_2=\left(n_j+\frac{1}{2}\right)D}\frac{dy_1dy_2}{\left\{\left(y_1-y_2\right)^2+\left[\left(n_i+\frac{1}{2}\right)D\right]^2+\left(n_kH\right)^2\right\}^{1/2}}+$$

$$\int_{x_1=a}^{x_1=0}\int_{x_2=\left(n_i+\frac{1}{2}\right)D}^{x_2=\left(n_i+\frac{1}{2}\right)D+a}\frac{dx_1dx_2}{\left\{\left(x_1-x_2\right)^2+\left[\left(n_j+\frac{1}{2}\right)D+a\right]^2+\left(n_kH\right)^2\right\}^{1/2}}+$$

$$\int_{x_1=a}^{x_1=0}\int_{x_2=\left(n_i+\frac{1}{2}\right)D+a}^{x_2=\left(n_i+\frac{1}{2}\right)D}\frac{dx_1dx_2}{\left\{\left(x_1-x_2\right)^2+\left[\left(n_j+\frac{1}{2}\right)D\right]^2+\left(n_kH\right)^2\right\}^{1/2}}\Bigg] \quad (13.b)$$

In calculating the integrals, n_k is even for the A-layers and odd for the B-layers.

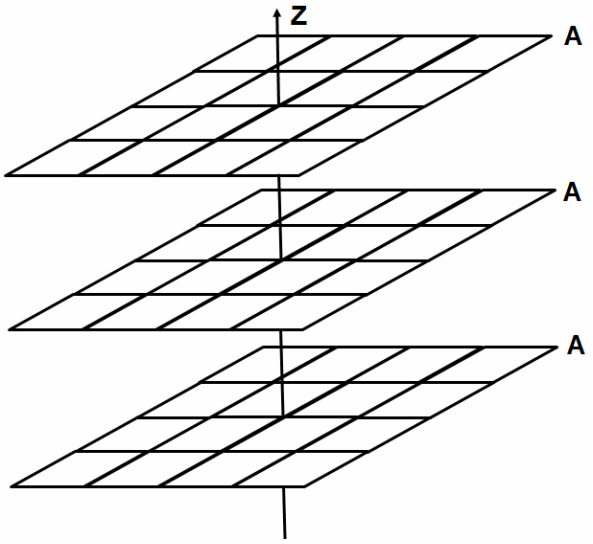

Fig. 7. AA stacking: the centers and vertices of the different layers are upon each other. In a word, the same layer (in two-dimension) repeats in third dimension with the same distance between layers.

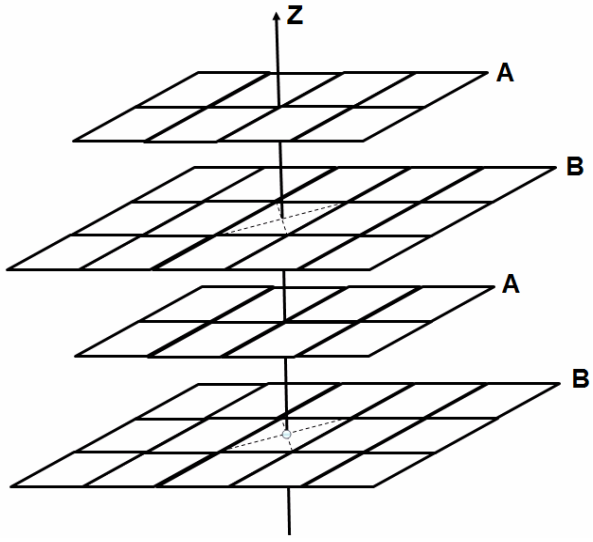

Fig. 8. AB stacking: the center of the one layer (B) is on the vertices of another layer (A) squares (4 squares) and vice versa.

The results are depicted in Figs. 9 and 10. It is observed that the distance between the layers of conducting rings plays a direct and crucial role in the magnitude of the total mutual inductance $\overline{M}_{3D}$ for both stacking patterns. For the AA stacking, we see regions where $\overline{M}_{3D}$ becomes even positive when the layers are close enough. In these regions, the overall

interaction between the rings becomes anti-ferromagnetic.

Though it is quite negligible, the total mutual inductance for the AB structure is larger in terms of magnitude than the AA structure. As a result the way of stacking layers is another influential factor in determining the total mutual inductance $\overline{M}_{3D}$ of the whole construction.

Another interesting behavior is the fact that once the layers are separated far enough, the way of stacking does not have any influence on the magnitude of the mutual inductance anymore and the behavior of the both patterns is the same [18], [22].

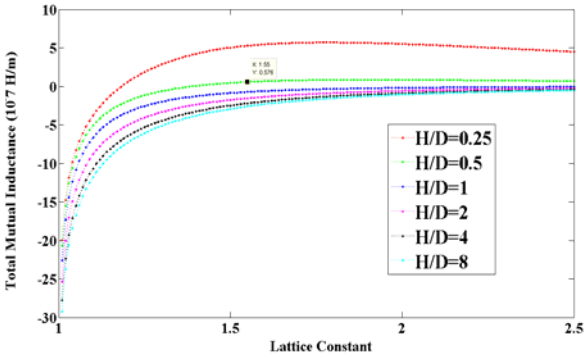

Fig. 9. The total mutual inductance for the AA stacking for different distances between the layers. When the ratio of this distance H to the lattice constant D is less than one (H/D=0.25, 0.5), there are regions where the total mutual inductance of the whole structure becomes positive. One of these points has been indicated.

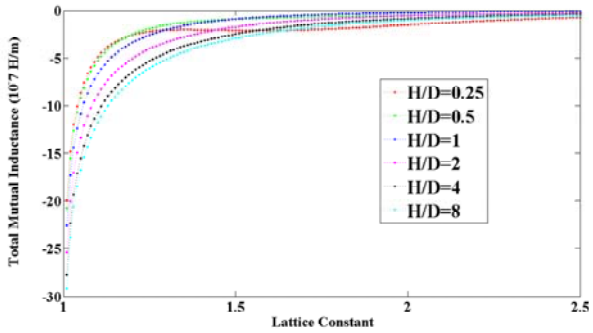

Fig. 10. The total mutual inductance for the AB stacking for different distances between the layers. In this layout, there is no region where the total mutual inductance becomes positive. Generally, this type of stacking leads to more negative mutual inductance.

B. Self-inductance

In the previous section, we have calculated the total mutual inductance of the square ring formation in two- and three-dimension. In order to obtain the second part contributing to the total magnetic flux, we have to consider the self-inductance L.

We must take the finite ring thickness into account since the self-inductance of an infinitesimal thin conductor with any geometry is infinite [12]. It is unlike the procedure of calculating the mutual inductance in which we have considered the infinitesimal thickness for wires. As a matter of fact, any thickness of the wire takes space away from the area which can be enclosed by the current and in turn decreases the captured magnetic flux. This case has been proved for the case of the circular ring architecture [18].

The energy of the magnetic field is stored inside and outside the wire. Hence it is necessary to calculate two contributions to the self-inductance: One part L_i generated by the interior field and the other part L_e caused by the exterior field. The second contribution is much larger than the first one. This is particularly true for our cases that the thickness of the wires is much smaller than the dimensions of the square. Another phenomenon that supports this approximation is the skin effect which forces the alternative current to stream on the surface of the conductor and consequently dwindles the magnetic flux inside the conductor. Here, the electric current flows mainly at the skin of the conductor between the outer surface and a level called the skin depth [12].

In the relevant literature, derivation of the relation for the self-inductance and its error has been elaborated for different geometries [27],[28]. For deriving the self-inductance due to the exterior field L_e, we use an indirect technique. It has been proved that the self-inductance of a wire loop could be written as a curve integral akin to the Neumann relation [27]. Accordingly, the expression for the external self-inductance of the square ring can be written as follows:

$$L_e = \frac{\mu_0}{4\pi}\Bigg[\int_{y_1=0}^{y_1=a}\int_{y_2=t}^{y_2=a-t} \frac{dy_1 dy_2}{\left[(y_1-y_2)^2+t^2\right]^{1/2}} + \int_{y_1=0}^{y_1=a}\int_{y_2=a-t}^{y_2=t} \frac{dy_1 dy_2}{\left[(y_1-y_2)^2+(a-t)^2\right]^{1/2}} + \int_{x_1=0}^{x_1=a}\int_{x_2=t}^{x_2=a-t} \frac{dx_1 dx_2}{\left[(x_1-x_2)^2+t^2\right]^{1/2}} + \int_{x_1=0}^{x_1=a}\int_{x_2=a-t}^{x_2=t} \frac{dx_1 dx_2}{\left[(x_1-x_2)^2+(a-t)^2\right]^{1/2}} + \int_{y_1=a}^{y_1=0}\int_{y_2=t}^{y_2=a-t} \frac{dy_1 dy_2}{\left[(y_1-y_2)^2+(a-t)^2\right]^{1/2}} + \int_{y_1=a}^{y_1=0}\int_{y_2=a-t}^{y_2=t} \frac{dy_1 dy_2}{\left[(y_1-y_2)^2+t^2\right]^{1/2}} + \int_{x_1=a}^{x_1=0}\int_{x_2=t}^{x_2=a-t} \frac{dx_1 dx_2}{\left[(x_1-x_2)^2+(a-t)^2\right]^{1/2}} + \int_{x_1=a}^{x_1=0}\int_{x_2=a-t}^{x_2=t} \frac{dx_1 dx_2}{\left[(x_1-x_2)^2+t^2\right]^{1/2}} \Bigg] \quad (14)$$

In the above equations, t represents the thickness of the wire. The error of this evaluation is of the first order in the wire thickness (square has four sharp corners) [27]. The function L_e is illustrated in Fig. 11. In this figure, it is demonstrated that as the thickness decreases, its self-inductance increases.

C. The Magnetic Permeability

Firstly, we describe the calculation of the mutual inductance M_{ij} between two infinitesimal square thin rings. By obtaining the total mutual and self inductance of the structure, it is possible to present the macroscopic magnetic response by calculating the magnetic permeability μ derived by Eq. (3).

In this work, it is presumed that the resistance of the wire material is negligible, i.e. R=0. So, the relative magnetic permeability μ_r is reduced to the following equation:

$$\mu_r = 1 + \chi_m = 1 - \mu_0 \frac{A_{ring}^2}{v} \frac{1}{L + \overline{M}} \quad (15)$$

By considering AB stacking, it is inferred that the appropriate lattice for this pattern is the bod-centered tetragonal (BCT) which its primitive cell volume is equal to D^2H.

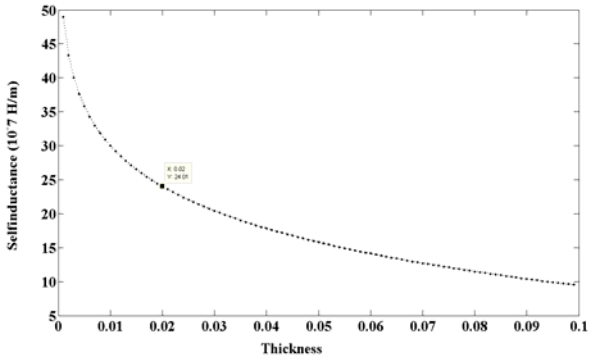

Fig. 11. The variation of the self-inductance of a square ring versus its thickness. The specified point is the value of the thickness and corresponding self-inductance used for succeeding calculations.

By knowing the area of the square ring $A_{ing}=a^2$, it is time to insert all the necessary ingredients in the equation above and end up with the following expression for the relative permeability μ_r:

$$\mu_r = 1 - \mu_0 \frac{a^4}{HD^2} \frac{1}{L_e + \overline{M}} = 1 - \mu_0 \frac{1}{(R)\left(\frac{D}{a}\right)^3} \frac{1}{\left(\frac{L_e}{a} + \frac{\overline{M}}{a}\right)} \quad (16)$$

where R is the ratio of the height of the unit cell H to the lattice constant D, i.e $R=H/D$. As mentioned earlier, all the lengths are scaled with the side of the square ring a. This scaling is employed in the final outcomes, too.

In Figs. 12 and 13 the relative permeability μ_r is plotted versus the lattice parameter for different heights of the unit cell H. It is noticeable that a dense packing of the cell

layers and the cells themselves reduces the relative permeability μ_r (its magnitude grows).

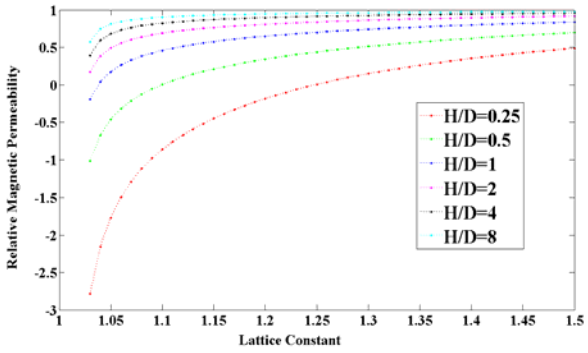

Fig. 12. There relative magnetic permeability for the AA stacking for different distances between the layers. Negative values for relative permeability up to -2.5 can be attained by close-packing of the cells.

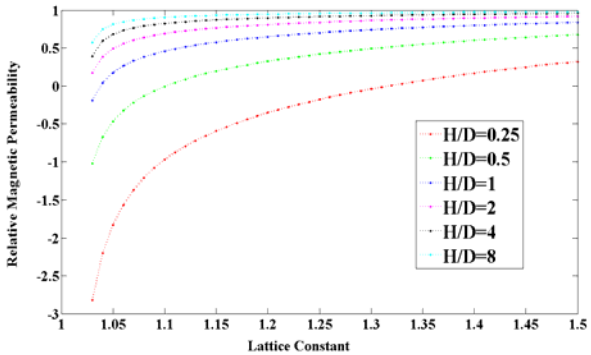

Fig. 13. There relative magnetic permeability for the AB stacking for different distances between the layers. The behavior of this pattern is very similar to the AA stacking (their difference is negligible).

In order to lessen the relative permeability μ_r, the denominator in Eq. (16) should be decreased as much as possible. By focusing on the denominator of Eq. (16), it is deduced that three ratios determine permeability: $R=H/D$, D/a and $(L+\overline{M})/a$. All of these factors can be reduced by low packing of the building cells. As the ratios H/D and D/a lesson, the sum $(L+\overline{M})/a$ also minimizes due to the fact that total mutual inductance becomes more negative and becomes comparable to self-inductance. Albeit there are regions for which the mutual inductance becomes positive (anti-ferromagnetic response for the AA stacking illustrated in Fig. 9, the magnetic permeability is again reduced when the layers are stacked close enough. Thus, it is of great importance to select the most appropriate values for these parameters to reduce the magnetic permeability a much as possible.

IV. Conclusion

We proposed the macroscopic properties of the conducting square ring configuration. We focused on the potential of the circulating currents in the current research. We analyzed the microscopic processes of self- and mutual-inductances of two- and three-dimensional ring systems. So, the self- and total mutual inductance of our design were calculated in the first step. Then, we applied a suitable averaging procedure to make appropriate predictions about the magnetic response of the structure.

References

[1] D.R. Smith, W.J. Padilla, D.C. Vier, S.C. Nemat-Nasser, and S. Schultz, "Composite medium with simultaneously negative permeability and permittivity," *Phys. Rev. Lett.*, vol. 84, pp. 4184-4187, 2000.

[2] R.A. Shelby, D.R. Smith and S. Schultz, "Experimental verification of a negative index of refraction," *Science*, vol. 292, pp. 77-79, 2001.

[3] S.A. Ramakrishna, "Physics of negative refractive index materials," *Rep. Prog. Phys.*, vol. 68, pp. 449-521, 2005.

[4] *Metamaterials: Physics and Engineering Explorations,* N. Engheta and R.W. Ziolkowski, Eds. IEEE Press, Piscataway, NJ, 2006.

[5] R.W. Ziolkowski and E. Heyman, "Wave propagation in media having negative permittivity and permeability," *Phys. Rev. E*, vol. 64, pp. 056625 (1-15), 2001.

[6] A. Taflove and S.C. Hagness, *Computational Electrodynamics: The Finite-Difference Time-Domain Method,* 3rd ed. Artech House, Inc. Norwood, MA, 2005.

[7] Y. Hao and R. Mittra, *FDTD Modeling of Metamaterials: Theory and Applications,* Artech House, Inc. Norwood, MA, 2005.

[8] J.B. Pendry, A.J. Holden, D.J. Robbins, and W.J. Stewart, "Magnetism from conductors and enhanced nonlinear phenomena," *IEEE Trans. Microwave Theory Tech.* vol. 47, pp. 2075-2084, 1999.

[9] R.E. Camley and D.L. Mills, "Surface polaritons on uniaxial antiferromagnets," *Phys. Rev. B*, vol. 26, pp. 1280-1287, 1982.

[10] L. Remer, B. Luthi, H. Sauer, R. Geick, and R.E. Camley, "Nonreciprocal optical reflection of the uniaxial anti-ferromagnet MnF2," *Phys. Rev. Lett.*, vol. 56, pp. 2752-2754, 1986.

[11] T. Dumelow, R.E. Camley, K. Abraha, and D.R. Tilley, "Nonreciprocal phase behavior in reflection of electromagnetic waves from magnetic materials," *Phys. Rev. B*, vol. 58, pp. 897-908, 1998.

[12] L. D. Landau, L.P. Pitaevskii and E.M. Lifschitz, "Electrodynamics of Continuous Media," in *Course of Theoretical Physics*, 2nd ed. vol. 8, Butterworth-Heinemann, 1984.

[13] P. Markos and C.M. Soukoulis, "Numerical studies of left-handed materials and arrays of split ring resonators," *Phys. Rev. E*, vol. 65, pp. 036622 (1-8), 2002.

[14] S. Linden, C. Enkrich, M. Wegener, J. Zhou, T. Koschny, and C. M. Soukoulis, "Magnetic response of metamaterials at 100 terahertz," *Science*, vol. 306, pp. 1351-1353, 2004.

[15] K. Aydin, I. Bulu, K. Guven, M. Kafesaki, C. M. Soukoulis, and E. Ozbay, "Investigation of magnetic resonances for different split-ring resonator parameters and designs," *New J. Phys.* vol. 7, pp. 168 (1-15), 2005.

[16] A.A. Zharov, I.V. Shadrivov, and Y.S. Kivshar, "Nonlinear properties of left-handed metamaterials," *Phys. Rev. Lett.* vol. 91, pp. 037401 (1-4), 2003.

[17] J.O. Dimmock, "Losses in left-handed materials," *Opt. Express*, vol. 11, pp. 2397-2402, 2003.

[18] M. Gorkunov, M. Lapine, E. Shamonina, and K.H. Ringhofer, "Effective magnetic properties of a composite material with circular conductive elements," *Eur. Phys. J. B*, vol. 28, pp. 263- 269, 2002.

[19] J.B. Pendry, A.J. Holden, W.J. Stewart, and I. Youngs, "Extremely low frequency plasmons in metallic mesostructures," *Phys. Rev. Lett.* vol. 76, pp. 4773-4776, 1996.

[20] J.B. Pendry, A.J. Holden, D.J. Robbins, and W.J. Stewart, "Low frequency plasmons in thin-wire structures," *J. Phys.: Condens. Matter*. vol. 10, pp. 4785-4809, 1998.

[21] E.N. Economou, T. Koschny, and C.M. Soukoulis, "Strong diamagnetic response in split-ring-resonator metamaterials: Numerical study and two-loop model," *Phys. Rev. B*, vol. 77, pp. 092401 (1-4), 2008.

[22] M. Lapine, A.K. Krylova, P.A. Belov, C.G. Poulton, R.C. McPhedran, and Y.S. Kivshar, "Broadband diamagnetism in anisotropic metamaterials," *Phys. Rev. B*, vol. 87, pp. 024408 (1-7), 2013.

[23] J.R. Reitz, F.J. Milford, and R. W. Christy, *Foundations of Electromagnetic Theory*, 4th Ed. Addison-Wesley, 2008.

[24] J.D. Jackson, *Classical Electrodynamics*, 3rd Ed. John Wiley and Sons Inc. 1999.

[25] C. Kittel, S. Fahy, and S.G. Louie, "Magnetic screening by a thin superconducting surface layer," *Phys. Rev. B*, vol. 37, pp. 642-643, 1988.

[26] A.K. Sarychev and V.M. Shalaev, "Electromagnetic field fluctuations and optical nonlinearities in metal-dielectric composites (Review article)", *Phys. Rep.* vol. 335, pp. 275-371, 2000.

[27] C.R. Paul, *Inductance: Loop and Partial*, 3rd Ed. John Wiley and Sons Inc. 2008.

[28] F. W. Grover, *Inductance Calculations: Working Formulas and Tables*, Dover Publications, Inc. Mineola, NY, 2009.

Amir Khodamohammadi was born in malekan, Iran, in 1978. He received the B.S. degree in physics from University of Tabriz Iran, with the best rank in 2000, and the M.S. degree in physics from the Valiasr University, Rafsanjan, Iran, in 2003. He is currently working toward the Ph.D. degree at the College of Optics and Photonics, University of Tabriz.

Since 2003, he has been working in Bonab Branch, Islamic Azad University. He is currently working on photonic liquid crystals and meta-materials theoretically and experimentally.

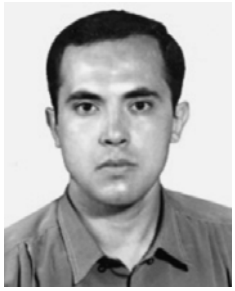

Ahmad Khayat Jafari, was born in Tehran, Iran, in 1978. He received the B.S. degree in physics from Isfahan University of Technology (IUT), Isfahan, Iran, with the best rank in 2000, and the M.S. degree in photonics from the Shahid Beheshti University (SBU), Tehran, Iran, in 2003. He is currently working toward the Ph.D. degree at the Department of Physics at the University of South Florida (USF).

Reza Aghbolaghi was born in Tabriz, Iran, in 1980. He received the B.S. degree in physics from University of Tabriz, Tabriz, Iran, in 2002 and the M.S. degree in photonics from the Shahid Beheshti University (SBU), Tehran, Iran, in 2005. He received the Ph.D. degree in laser physics from University of Guilan.He is currently working on meta-materials, photonic crystals, and attoscience theoretically and experimentally in University of Bonab. Additionally, he conducts numerical simulation in disk lasers. He also collaborates with the Disk Laser Group, Center of Laser Science and Technology (CLST), Tehran. There, his activities are in the field of laser development, investigation of laser/material interaction.

THIS PAGE IS INTENTIONALLY LEFT BLANK.